Spectroscopy of self-assembled quantum rings

R J Warburton[1], B Urbaszek[1], E J McGhee[1], C Schulhauser[2], A Högele[2], K Karrai[2], A O Govorov[3], J A Barker[4], B D Gerardot[5], P M Petroff[5], and J M Garcia[6]

[1]Department of Physics, Heriot-Watt University, Edinburgh EH14 4AS, UK
[2]CeNS and Sektion Physik, Ludwig-Maximilians-Universität, Munich, Germany
[3]Department of Physics and Astronomy, Ohio University, Athens, USA
[4]Cavendish Laboratory, University of Cambridge, Cambridge, UK
[5]Materials Department, University of California, Santa Barbara, USA
[6]Instituto de Microelectronica de Madrid, Madrid, Spain

Abstract. A summary is presented of optical spectroscopy measurements on self-assembled quantum rings. The rings are unusual quantum dots, having a pronounced hole in the centre, and can be self-assembled during growth using a modified Stranski–Krastanow procedure. We embed the quantum rings in a capacitor-like structure which enables us to load the quantum rings with electrons and to apply a vertical electric field. The results of these experiments, performed on a large number of individual quantum rings at low temperature, reveal pronounced Coulomb interactions and an excitonic Stark effect. Additionally, we have applied a magnetic field, primarily to probe the form of the lateral wave functions, but we find that this too yields insights into the Coulomb interactions. Model calculations are used to interpret these results.

1. Introduction

Self-assembly of quantum dots exploits the strain arising in the growth of lattice mismatched semiconductors, for instance InAs on GaAs. At our growth temperature, this process yields lens-shaped InAs quantum dots with a diameter and height of about 20 nm and 6 nm respectively. The In floats to the surface in this process so that the dots are entirely InAs at the top, and entirely GaAs at the bottom [1]. Capping with GaAs clearly destabilises the dots, leading to structural changes. Remarkably, under certain conditions ring-shaped structures can be produced, where the central hole is of comparable size to the original dot [2].

We have probed the properties of quantum rings with optical spectroscopy. Single dot spectroscopy has turned out to be vital, not only for the high spectral precision but also because the optical properties can differ widely from one ring to the next despite the apparent homogeneity in the topography. We have probed the nature of the excitonic wave functions by applying electric and magnetic fields, comparing the results to model calculations.

2. Growth and heterostructure design

The quantum rings are grown by first self-assembling InAs quantum dots on GaAs, and then by depositing 1 nm of GaAs, annealing for about 30 s at the growth temperature of 530°C. The atomic force micrograph in Fig. 1 shows how in this case all the dots have converted into rings. As shown in the profile, the radius measured at the position of maximum height is $\sim$ 15 nm, and the maximum height from the central hole is $\sim$ 4 nm. The rings extend to a radius of $\sim$ 50 nm. The ensemble photoluminescence (PL) spectrum contains two dominant peaks, one centred at 1.31 eV, the other at 1.34 eV, which we refer to the red and blue bands, respectively.

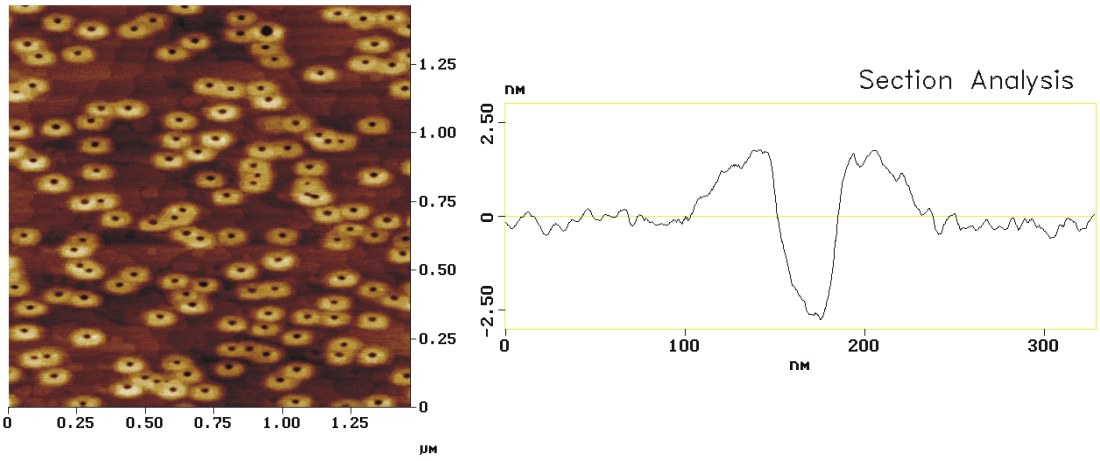

Figure 1. Left: An atomic force micrograph of uncapped quantum rings. The rings are elongated along the $[1\bar{1}0]$ direction. Right: a profile through the centre of a typical quantum ring.

There is also a weaker peak, on the red side of the red band. The origin of this multi-modal spectrum is unknown, but is most likely a multi-modal distribution in the vertical confinement.

We embed the quantum rings between an electron reservoir (n^+-GaAs, the back contact) and the sample surface. The rings are just 25 nm from the back contact allowing fast tunneling of electrons from the back contact into the dots, but tunneling to the surface is blocked by 150 nm of barrier material. Ohmic contacts are made to the back contact and a NiCr semi-transparent gate electrode is deposited onto the surface. The high doping in the back contact pins the Fermi energy close to the GaAs conduction band edge, and by changing the gate voltage V_g we can alter the position of the ring levels relative to the Fermi energy, allowing us to alter the charge state of the rings. There exists a pronounced Coulomb blockade such that the charge remains constant over large regions of V_g [3]. We present here measurements of the PL from individual quantum rings at 4.2 K. The PL is excited by generating carriers in the wetting layer with a pump wavelength between 820 and 850 nm. A magnetic field is applied along the growth direction (the [001] direction). The results of a typical experiment are shown in Fig. 2, a plot of the PL energy against V_g representing the PL intensity with a grey scale. At large and negative V_g, the PL is quenched because of electric-field induced ionisation, but at a particular V_g emission from the neutral exciton (X^0) appears. At more positive V_g, the PL abruptly red-shifts because the singly-charged exciton (X^{1-}) is now favoured. At higher V_g still the transition from X^{1-} to X^{2-} is observed. The X^{2-} shows a characteristic doublet because there are two possible final states split by the exchange energy [3]. The broadening at higher V_g is associated with the occupation of the wetting layer states with electrons.

3. Excitonic Stark effect

In the regions of V_g where the excitonic charge remains constant, the PL energy changes with electric field as a result of the Stark effect. We analyse this by subtracting the Coulomb energy shifts from the PL energy, and by converting V_g into an electric field [4]. We find that for all rings, the PL energy E_{PL} can be fitted convincingly to a quadratic function of the electric field, F: $E_{PL} = E_0 - erF + \beta F^2$, where r is the separation of the electron and hole wave functions and β is the polarizability. We find that both r and β change considerably from ring

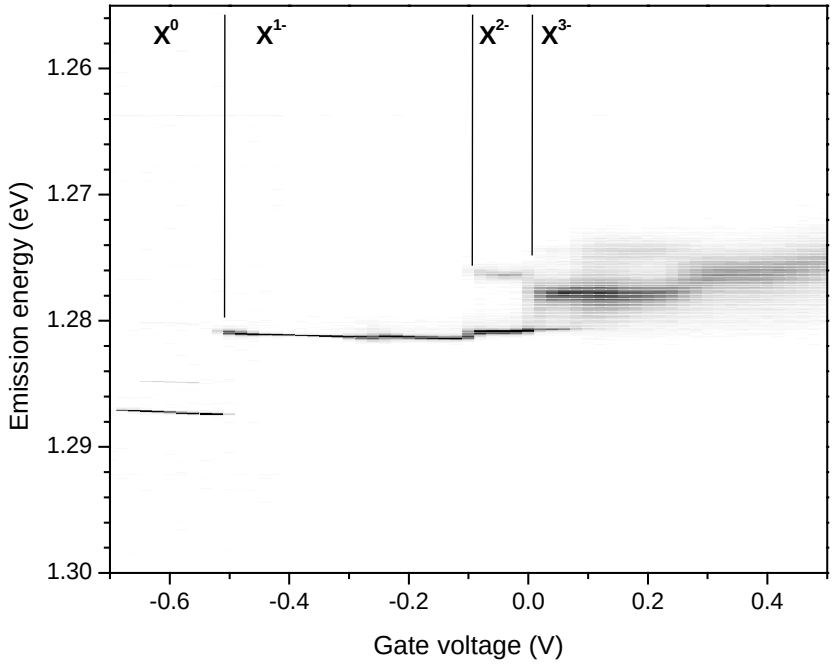

Figure 2. Emission energy against gate voltage for an individual quantum ring. The PL is represented by a grey scale: white represents the background signal and black 800 counts on the detector. The voltages at which the charge state of the exciton changes are marked.

to ring, but with a clear trend on the PL energy: the red-band rings have $r \sim -0.5$ nm and the blue-band rings $r \sim -2$ nm (Fig. 3). Despite the statistical fluctuations in r and β as a function of E_0, we find a close correspondence between r and β (Fig. 4).

The permanent dipole moment, on average -1.1 nm, is both opposite in sign and larger in magnitude than that for InAs quantum dots [5]. It corresponds to the case where the centre-of-gravity of the hole wave function is located *below* that of the electron. The magnitude is surprisingly large, comparable to the ring height. Hence, a clear result of these experiments is that the ring formation has changed drastically the electron and hole vertical confinement. The reduction in height on going from dots to rings cannot explain the result; instead, the large excitonic dipole moment is a consequence of both the change in shape and In migration.

Some insight into the linear relationship between r and β can be obtained by considering a parabolic vertical confinement potential with an in-built electric field F_0 to induce the excitonic dipole moment. In this case, $F_0 = -p/2\beta$. Hence, the result of the experiment is that each ring has almost the same in-built field. In turn, this implies that an exciton in each ring has roughly the same lateral area: if we represent the electron and hole wave functions as two plates (area A) of a capacitor, $F_0 = e/A\varepsilon_0\varepsilon_r$ (independent of the plate separation from Gauss' Law). The data for the quantum rings give an average $F_0 = -42$ kV/cm and $A = 360$ nm^2 with a standard deviation of just 12%. In detail, however, a plot of F_0 against E_0 shows a clear bunching into three groups, corresponding to the three distributions inferred from the ensemble PL (Fig. 4). For both the red and blue-band dots, F_0 tends to decrease, and A tends to increase, with increasing E_0.

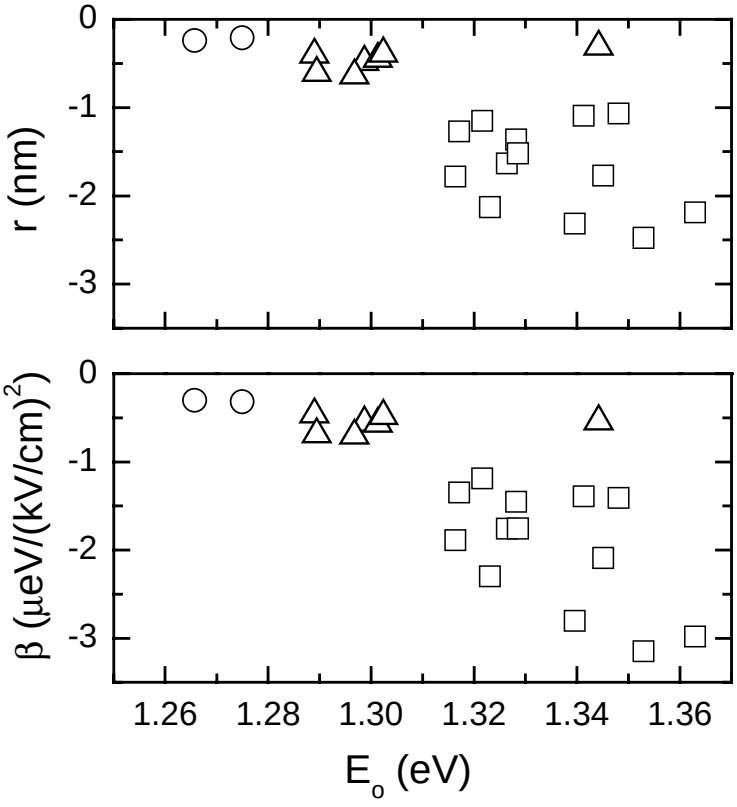

Figure 3. Excitonic permanent dipole moment, r, and polarizability, β, plotted against the maximum photoluminescence (PL) energy, E_0. Each point represents the result from one quantum ring. The symbol denotes the band to which each ring belongs.

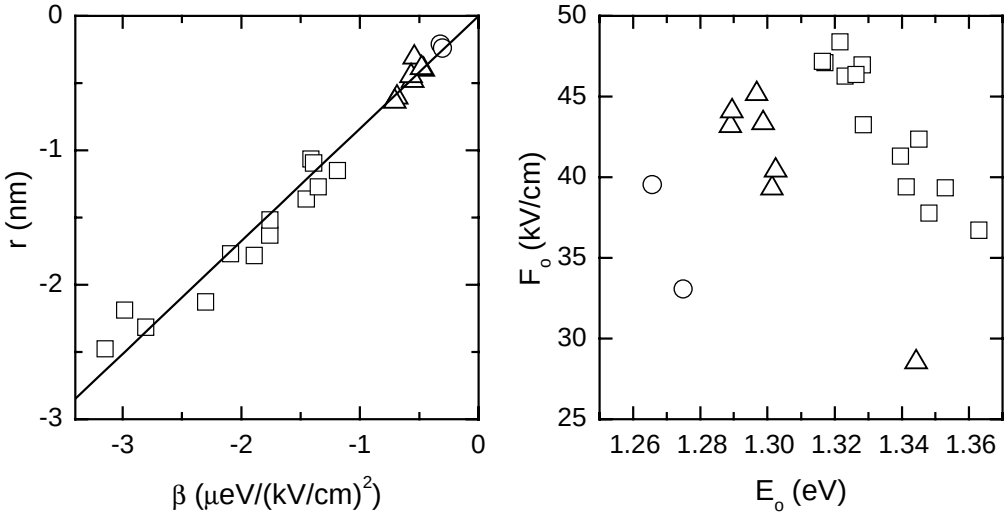

Figure 4. Left: the permanent dipole moment, r, versus the polarizability, β with a straight line fit. Right: the in-built electric field, $F_0 = -p/2\beta$, versus maximum PL energy, E_0, where, as in Fig. 3, each point represents a single ring, and where the symbol identifies the PL band.

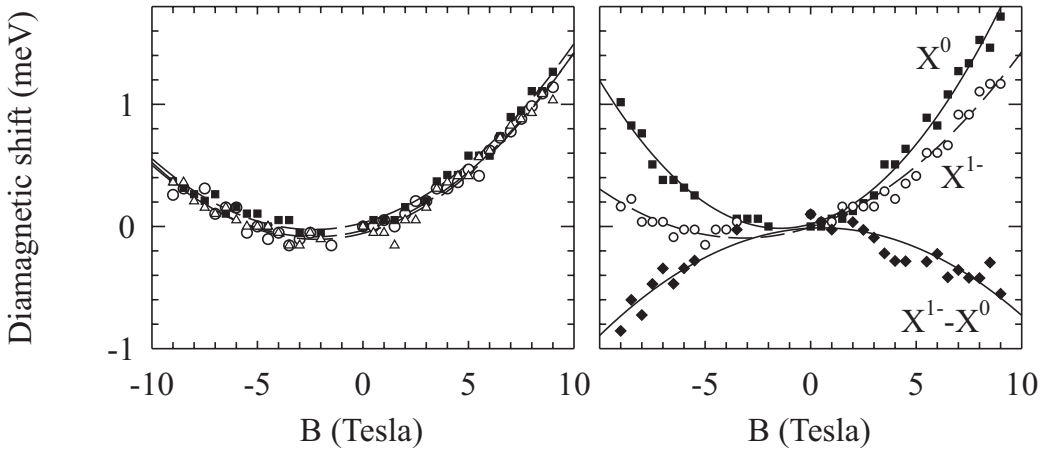

Figure 5. Left: the energy dispersion in magnetic field, B, of a red-band quantum ring, shown for the X^0, X^{1-}, and X^{2-} excitons. Right: the energy dispersion of a blue-band quantum ring for X^0 and X^{1-} excitons. The solid lines are 2nd order polynomial fits.

4. Diamagnetic shift

Measurement of the Stark shift produces only indirect information on the extent of the lateral wave function. In order to address this issue, we have applied a magnetic field as the diamagnetic curvature is proportional to the lateral excitonic area. We observe two branches in B, split by a linear Zeeman effect ($120\,\mu$eV/T). In order to extract the diamagnetic term, we plot the upper (lower) branch against positive (negative) B and fit the results to a parabola. Fig. 5 contains representative results for a red-band dot and a blue-band dot. For the red-band dot, the diamagnetic shift is $\alpha = 10\ \mu\text{eV/T}^2$, independent of the excitonic charge within our experimental uncertainty of $\sim 10\%$. Conversely, a blue-band dot has $\alpha = 16.6\,\mu\text{eV/T}^2$ for X^0, but a significantly lower $\alpha = 8.7\,\mu\text{eV/T}^2$ for X^{1-}. The latter result implies that charging induces a *paramagnetic* term to the susceptibility.

To comment on these results, we have performed model calculations, incorporating the Coulomb interactions between electrons and holes in a perturbation theory approach [6]. Taking a parabolic confinement potential we find that in this limit, appropriate to the red-band rings which have an excited state in the PL some 50 meV from the ground state, we reproduce the red-band diamagnetic curvature with an electron quantization energy of about 30 meV. With this confinement energy, the Coulomb interactions give a $\sim 30\%$ reduction in the diamagnetic curvature from the single particle limit, but the differences between X^0, X^{1-} and X^{2-} are less than $1\,\mu\text{eV/T}^2$. We expect this result on the importance of the Coulomb terms to be preserved also for other confinement potentials provided that the quantization energies are large. This explains the magnetic behaviour of the red-band rings. In contrast, the reduction in α on charging for the blue-band rings cannot be explained in this way. The corollary is that the blue-band rings are not in the strong confinement regime; we suggest that the blue-band excitons are in a regime where the single particle and Coulomb energies are comparable. In the extreme of weak confinement, a pronounced paramagnetism and the appearance of shake-up peaks in the PL can be expected, but these have not yet been observed.

A natural question is whether the ring-like topography leads to oscillations in B as flux quanta are threaded through the central hole. An exciton in a ring-like landscape represents a rich problem. Excitons in wide rings with equivalent electron and hole confinement potentials are not expected to show any flux-related oscillations [7,8], but this can change if the electron

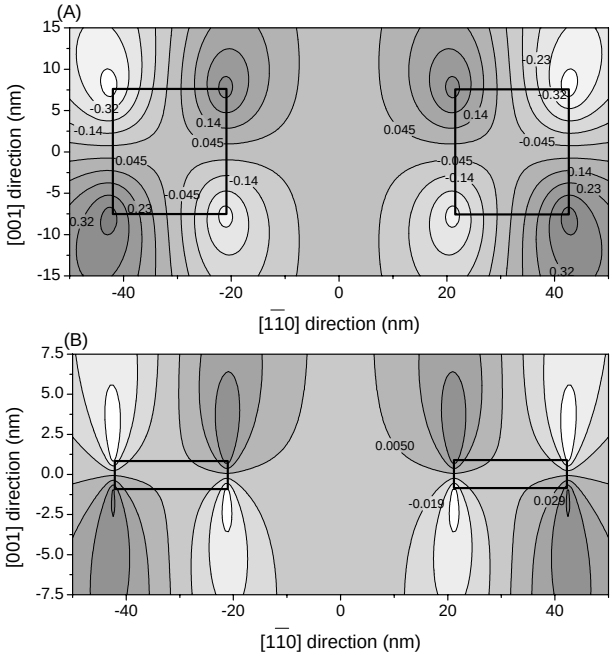

Figure 6. Piezoelectric potential distribution as a function of position on the (110) plane through the dot centre, for box-like InAs/GaAs quantum rings. In (A) the outer box dimensions are (60,60,15) nm and the inner dimensions are (30,30,15) nm; in (B) the outer box dimensions are (60,60,2) nm and the inner dimensions are (30,30,2) nm. The labels of the contours are in eV.

and hole are confined in different ways. If the hole is centrally confined with the electron free to orbit around the ring, the PL is predicted to quench above a certain magnetic field because the electronic ground state has a finite angular momentum [8, 9]. The PL is also predicted to quench when the electron and hole both propagate around the ring but with different radii as this rotating dipole also has a finite angular momentum in magnetic field [9]. In the present case, the majority of rings show a smooth energy dispersion in the PL up to our present limit 9 T with no evidence of quenching (according to the ring geometry, one flux quantum passes through the ring at about 6 T). However, a few rings have shown a change in diamagnetic curvature at about 6 T and this has been tentatively interpreted as a flux-related effect in a ring-like geometry [10]. This behaviour has not been predicted theoretically and a firmer statement on the experiments will only be possible with more experimental data.

5. Calculations of strain and piezoelectric field in quantum rings

We have calculated the electron and hole wave functions in ring-like nanostructures. The strain and the piezoelectric field are incorporated in a continuum model and a plane wave expansion is used to solve the Schrödinger equation for the system [11]. We assume that the central hole consists of pure GaAs and we take a variety of shapes and composition profiles for the rings. Despite the large parameter space, some general features emerge.

First, the piezoelectric field plays an important role. For a quantum dot, the maxima and minima of the piezoelectric potential are located outside the dot [12], yet the wave functions for both electrons and holes are localised inside the dot, such that the piezoelectric field plays a very minor role for the ground states. For a ring, however, the strained core generates an additional piezoelectric potential which has a stronger interaction with the carriers inside the ring, as illustrated in Fig. 6. The piezoelectric potential breaks the rotational symmetry, and

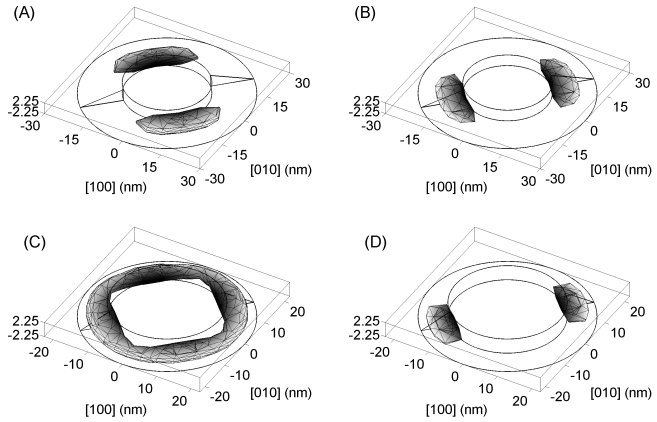

Figure 7. Surface plots of probability densities, $|\psi(\mathbf{r})|^2$, plotting the contour at 50% of the peak probability density. (A) The ground state electron wave function in an InAs/GaAs quantum ring of inner radius 15 nm, outer radius 30 nm, and maximum height 4.5 nm. (B) The ground state heavy hole wave function for the ring shape considered in (A). (C) The ground state electron wave function in a ring with a similar geometry to (A) but with a 22.5 nm outer radius. (D) The ground state heavy hole wave function for the ring shape considered in (C).

results in maxima in the electron confinement with associated minima in the hole confinement every 180° as a carrier propagates around the ring. For the tall ring in Fig. 6A, the piezoelectric potential minima/maxima can be as large as ± 0.5 eV. For rings with a large aspect ratio, such as the self-assembled rings, the piezoelectric potentials are substantially smaller with maxima and minima outside the ring (Fig. 6B). Nevertheless, the piezoelectric effect gives rise to a pronounced angle-dependent potential which tends to separate the electrons and holes both vertically and laterally.

Secondly, for shapes and compositions that are plausible representations of the self-assembled quantum rings, the holes are localised in the $(1\bar{1}0)$ plane passing through the centre of the ring. This is entirely due to the piezoelectric potential. Additionally, the self-assembled rings are elongated such that the hole localisation is enhanced. Although the material in the ring centre is biaxially strained, which represents an attractive potential for the holes, we find that this is a modest effect for our large aspect ratio rings. The real rings are not of course perfectly symmetrical, and so either the [110] or $[\bar{1}\bar{1}0]$ direction will be energetically favoured. In the light of this, it is therefore likely that the holes are localised and are not free to propagate around the ring.

Thirdly, the nature of the electron states is very sensitive to the details of the structure. For instance, for large volume rings where the piezoelectric potential is very strong, the electron wave function is localised in the (110) plane, orthogonal to the holes. For smaller volume rings where the piezoelectric potential is weaker, the electron wave function extends around the ring. And finally, for sufficient extension along the [110] direction, the electron can be localised with the hole in the $(1\bar{1}0)$ plane. Two examples are shown in Fig. 7.

We have analysed a variety of structures which are compatible with the topology from the AFM to find if we can reproduce the results of the optical spectroscopy, namely a large electron-hole overlap and a large electron–hole dipole moment. Assuming GaAs barriers on all sides, we find that the ring must be more than 2 nm high in order to explain the large dipole moments simply because the electron–hole separation can be at most about half the vertical height, even when allowing for extreme indium composition profiles. We therefore consider a conical cross-section with a maximum height of 4.5 nm at a radius of 15 nm. We find that the holes are pulled to the bottom of the ring by the confinement in the conical shape, and

are localised in the $(1\bar{1}0)$ plane passing through the ring centre by the piezoelectric potential. If the electrons are pulled toward the top of the ring by the piezoelectric potential we have a natural explanation for the large dipole moment. We suggest therefore that the electrons must be localised towards the rim of the ring so that the piezoelectric field pulls the electrons to the top of the structure. This will arise either by having a small volume ring (see Fig. 7) or by an indium concentration gradient where the In content is large at the rim of the ring, and small at the outer edge. The latter possibility has been suggested from considerations of the ring formation [13]. If the piezoelectric field is very strong, then the overlap between the electron and hole wave functions is small (Fig. 7), contrary to the experimental results. However, for a given ring height, we find the largest dipole moments for structures where the electron wave function is delocalised, and furthermore, the ring elongation will enhance the electron-hole wave function overlap. While the suggested structure (Fig. 7C and D) is by no means the only possibility, we believe that it contains the necessary ingredients to account for the experimental results.

6. Discussion

Optical spectroscopy on self-assembled quantum rings has revealed some striking effects. On average, the electron and hole wave functions are separated by about 1 nm with the hole localised toward the base of the ring, the electron toward the top. While there is a large variation in dipole moment from ring to ring, there is a close linear relationship between the dipole moment and the polarizability. We have argued that the piezoelectric field is important for quantum rings and is a likely mechanism for the vertical separation of the electron and hole. At this stage electronic structure calculations cannot offer a detailed description of the quantum rings because the exact shape and composition profile are unknown. However, it is very likely that the holes are localised in the $(1\bar{1}0)$ plane passing through the ring centre, pulled to the base of the rings by the piezoelectric field. The electron wave functions are very dependent on the details of the structure and this might be the explanation for the wide spread in dipole moment, despite the apparently small fluctuations in the topography from one ring to the next. In experiments in a magnetic field, we find limited evidence for the quantization of flux in the excitonic spectra. A natural explanation for this is the localisation of the exciton somewhere in the $(1\bar{1}0)$ plane, primarily caused by the condensation of the hole wave function. The challenge for the future is to relate optical spectroscopy, structural information and model theory more closely together. The motivation is to reveal new physics and to provide a framework for designing semiconductor nanostructures with particular properties.

References

[1] Kegel I *et al* 2000 Phys. Rev. Lett. 85 1694
[2] Garcia J M *et al* 1997 Appl. Phys. Lett. 71 2014
[3] Warburton R J *et al* 2000 Nature 405 926
[4] Warburton R J *et al* 2002 Phys. Rev. B 65 113303
[5] Fry P W *et al* 2000 Phys. Rev. Lett. 84 733
[6] Warburton R J *et al* 1998 Phys. Rev. B 58 16221
[7] Song J and Ulloa S E 2001 Phys. Rev. B 63 125302
[8] Galbraith I, Braid F J, and Warburton R J 2002 Phys. Stat. Sol. (a) 190 781
[9] Govorov A O, Kalameitsev A V, Warburton R, Karrai K, and Ulloa S E 2002 Physica E 13 297
[10] Haft D *et al* 2002 Physica E 13 165
[11] Barker J A and O'Reilly E P 2000 Phys. Rev. B 61 13840
[12] Davies J H 1998 J. Appl. Phys. 84 1358
[13] Lorke A *et al* 2002 Mat. Sci. Eng. B88 225